Quantification of Resistance and Bandwidth-Correlated Noise in Linear Electronic Components

Grant Saggars*
University of Kansas
(Dated: March 8, 2025)

It had been known in Johnson's time that the characteristic noise of linear electronics, attributed to statistical mechanical effects, was a function of bandwidth and resistance, and was white in nature. We attempt to replicate Johnson's original work using an array of modern amplifiers and band pass filters to assess the resistance and frequency correlation in this noise, which has come to be known as Johnson noise. We conclude with high certainty that resistance and bandwidth dependences are linearly correlated, and use these results to provide a strong estimate of Boltzmann's constant.

I. INTRODUCTION

It has been widely observed that there exists approximately white noise as electronic fluctuations within resistive materials. Amplifier technicians in the early 20th century first noticed that a small fraction of noise persisted independently of the then-called "tube noise." Johnson first experimentally measured this quantity in 1926, where it was found that it is proportional to both resistance and frequency. This experiment also provides a delightful way to measure Boltzmann's constant, despite Johnson's original work scraping by with a 13% error on this for the time [1]. It is predicted that Johnson noise is proportional to total frequency bandwidth and resistance, given by:

$$V_{\text{RMS}} = \sqrt{4k_B T \Delta F}$$

Johnson noise is typically in the regime of 1×10^{-6} V. To measure noise on such small scales, I repeat the method of Johnson's original work, using TeachSpin's "Noise Fundamentals" equipment [2]. In the same light as the original work, a pre and post amplifier, coupled with a squarer on the voltage output, shown in figure 1. Bandwidth and resistance dependence are reviewed, and results used to compute Boltzmann's constant.

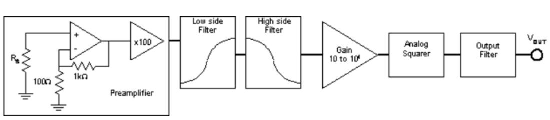

FIG. 1. Schematic of the instrumentation. Sample resistance can be controlled in the preamplifier stage, where a fixed gain of 600x is applied. This is fed into two filters, high and low pass effectively forming a band-pass. This is fed through a primary gain, which is configured to minimize clipping in measurement. Finally, this is passed through an analog squarer and output filter, which takes a time-average.

The nature of Johnson and amplifier noise is approximately white; in that the time average for all but terahertz frequencies is zero [1]. Consequently, we employ an analog voltage squarer, which has advantages in The output of the amplification stage introduces amplifier noise several orders larger magnitude than Johnson noise of the system, however it is possible to separate the two as a consequence of the squarer, where in a time averaged regime, uncorrelated voltage sources (noise) with gain G can be superimposed as in equation 1. This establishes the RMS amplifier noise, which is then subtracted off.

$$\langle V_{\text{out}}^2 \rangle = G^2 \left[\langle V_J \rangle + \langle V_N \rangle \right]^2 = G^2 \left[\langle V_J^2 \rangle + \langle V_N^2 \rangle \right] \quad (1)$$

II. RESISTANCE AND FREQUENCY DEPENDENCE

A. Experimental Setup

In the resistance dependency measurements, we take measurements using octave scale resistors provided by TeachSpin manufacturers, from 1 Ω to 100 $k\Omega$ (tolerance 0.1%). This is supplemented with metal film resistors (tolerance 0.1%) which can be directly measured using a Fluke 179 Multimeter. We label these BEXT and CEXT, and have corresponding resistances which can be found in table I. Our configuration uses a preamplifier, filter, secondary amplifier, squarer, and time-averager. The first stage in the pre-amp has a set gain of $g = 1 + R_f/R_1$, where $R_f = 1\ k\Omega$ and $R_1 = 200\ \Omega$. This is fed through a hard-wired amplifier with gain 100, set by a similar ratio of resistor values. Our filters are a separately configurable high and low pass filter, approximated well by the Butterworth response, with damping parameter $\gamma = \frac{1}{2Q}$. These considerations are significant in the determination of frequency dependence in Johnson noise. For more information about the equivalent bandwidths, see table II C This is then fed through the secondary amplifier, which we configure to eliminate signal clipping while providing a sufficient boost in signal, and follow the same uncertainty as with the preamplifier. Output is passed to a squarer, which is subject to zero-offsets; however, the static squaring accuracy is claimed to be about 0.2% with a bandwidth that extends to 3 MHz. The time-average of this is fed through to a Fluke 179 multimeter. We opt for a time constant of $\tau = 0.1$ s.

* Grant-S@ku.edu

Resistor	Resistance
1	1.0 Ω
2	10.0 Ω
3	100.0 Ω
4	1000.0 Ω
5	10000.0 Ω
6	100000.0 Ω
BEXT	279.9 Ω
CEXT	2996.0 Ω

TABLE I. Resistor Values.

B. Separation of Noise & Resistance-Correlation of Johnson Noise

Johnson predicts his noise is proportional to resistance, and to confirm this we systematically fix the bandwidth while varying resistance. We selected 100 Hz on the high pass filter, and 10 kHz on the low pass filter for an effective bandwidth of 10,996 Hz (see table II C for values) by modeling our filters using the Butterworth response model. We then vary the resistor by switching between 1 Ω to 100 $k\Omega$ in octave steps.

The noise induced by our amplifier is many times larger than the Johnson noise, and must therefore be separated from the signal. This can be done because the mean-square voltages from uncorrelated sources are additive. We accomplish this by extrapolating to the zero resistance regime by fitting a linear curve, wherein only amplifier noise is measured, shown in figure 2.

We collected two datasets at different gain, and determined that there is a substantial error at higher gain. We compensate for this by using data at 6000 gain only for resistances below 0.1 $k\Omega$. Gain of 1500 was used in all other ranges, which sacrifices precision at low resistances, but does not suffer from clipping at high resistance.

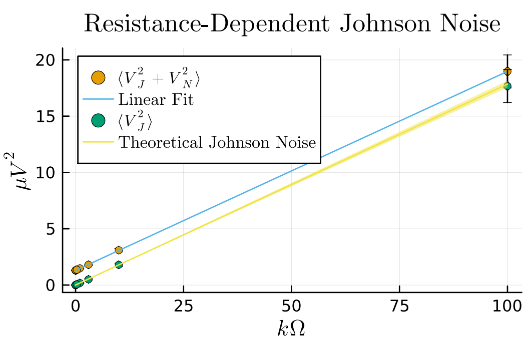

FIG. 2. Output collected from the time-averager, shown in blue, is fit to a linear curve to extrapolate in the $R \to 0$ regime such that amplifier noise can be extracted. The resulting data, $\langle V_J^2 \rangle$, is plotted in green, and the theoretical prediction made by Johnson's model overlaid in yellow.

Figure 2 shows that resistance-dependence in Johnson noise is fit exceptionally well by Johnson's model. We find a chi-squared value per degree of freedom of 0.11, which is to say that the observed scatter is less than that predicted by the analytical uncertainties.

C. Bandwidth-Correlation of Johnson Noise

Johnson's model also predicts a proportionality to bandwidth in the magnitude of noise. Following the separation of amplifier noise from Johnson noise, we can directly subtract off the amplifier noise from the value measured out of the time-averager (time constant of 0.1 s). In doing so, we can now vary the bandwidth while letting resistance remain at a fixed 10 $k\Omega$. We systematically adjust the high and low pass filter to the values seen in table II C.

In our analysis of the data, we found it incredibly important to model the frequency rolloff of the gain function. Amplifier gain is not constant across frequencies, and it typically follows a transfer function, such as:

$$G(f) = G_0 \cdot H(f)$$

In our case, the transfer function is modelled well as

$$H(f) = \frac{1}{\sqrt{1 + \left(\frac{f}{f_c}\right)^4}}$$

Previously, our gain was said to be the product of preamp and primary gain. This was an acceptable approximation in the previous sections, because the difference in theoretical cutoff frequency was very close to the actual cutoff frequency, making this a very small correction term; however, this is not necessarily the case in our assessment of frequency-correlated measurements, particularly in the larger bandwidths.

Because we chose to separate amplifier noise at a particular bandwidth in the resistance-correlated measurements, we cannot reuse the amplifier noise measurement as it depends on parameters in the high and low pass filters. Instead, we fit our frequency-correlated dataset to the zero-bandwidth regime to equivalently separate amplifier noise in the same fashion.

	0.33 kHz	1 kHz	3.3 kHz	10 kHz	33 kHz	100 kHz
10 Hz	355.0	1100	3654	11096	36643	111061
30 Hz	333.0	1077	3632	11074	36620	111039
100 Hz	258.0	1000	3554	10996	36543	110961
300 Hz	105.0	784	3332	10774	36321	110739
1000 Hz	9.0	278	2576	9997	35543	109961
3000 Hz	0.4	28	1051	7839	33324	107740

TABLE II. Effective bandwidths from the high pass (leftmost column) and low pass (upper row) parameters.

D. Noise Density

In the previous sections, we found a linear correlation in frequency and resistance for Johnson noise. Using these relations, we define a noise density in frequency, $\langle V_J^2 \rangle / \Delta f$. This allows us to parameterize noise density with a single value, R. Doing so provides a complete summary of our results, shown in figure 3.

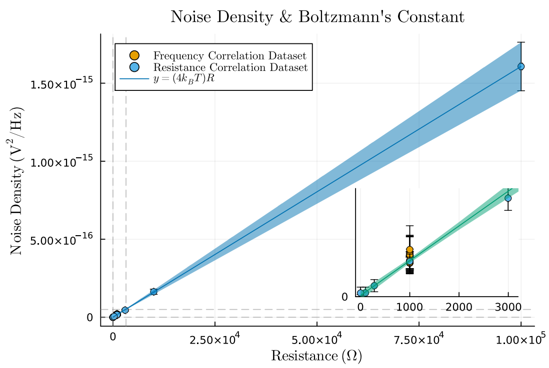

FIG. 3. It's predicted that Johnson noise is linearly correlated with both noise and frequency, so by constructing a "density" in the squared voltage per bandwidth, it is possible to directly fit a value for Boltzmann's constant. In this case, we find a value of $1.33 \times 10^{-23} \pm 1.34 \times 10^{24}$ J/K. In Johnson's original work, k_B was found to be significantly lower at $k_B = 1.27 \times 10^{-23} \pm 13\%$ J/K. Since 2020, the accepted value for k_B has been 1.380×10^{-23} J/K, placing our mean under 4% of the accepted value.

III. DISCUSSION

In this paper, we demonstrate the linear correlation in frequency and resistance for Johnson noise, and in doing so we fit a value for Boltzmann's constant, $k_B = 1.33 \times 10^{-23} \pm 1.30 \times 10^{-24}$. The associated z-score of this is -0.376, suggesting my data models the now accepted value for Boltzmann's constant well. The exceptionally low chi-square value suggests that this could be improved further with more data, to observe the spread of data more completely.

Appendix A: Discussion of Precision and Uncertainty

Throughout this work, we use linear propagation theory for the propagation of all errors via the excellent measurements library in Julia [3].

We perform several standard statistical assessments of our data, necessary for chi-square testing. First, uncertainty is propagated. For a comparison of systematic uncertainties, see table IV. Statistical uncertainty originates exclusively from the time-averager. We select a time constant (τ) of 0.1 s and a period of 10 s. Number of samples is effectively given as:

$$N = \frac{T}{\pi \tau}$$

Given that Johnson noise is white (unbiased) in nature, we consider a standard deviation from this to be:

$$\sigma_{\text{stat}} = \frac{1}{\sqrt{N}}$$

The squares of systematic and statistical uncertainty may be added. We found a chi-square value for resistance-correlation and frequency-correlation measurements in the standard fashion:

$$\frac{\chi^2}{\text{NDOF}} = \frac{1}{\text{NDOF}} \sum \frac{V_{\text{meas}}^2 - V_{\text{theoretical}}^2}{\sigma^2}$$

Where NDOF is the quantity of resistance data points minus one. A summary of results can be found in table III. We found low chi-squared values for all except the frequency dependent regime, which suggest larger errors than theoretically predicted. The frequency-dependent regime is unique, in that there is substantial variation in low bandwidth values as a result of large variation in output in electronic components. It may be beneficial to wait longer between measurements using the same time constant, as this can reduce uncertainty significantly for high resistance, much more than even order of magnitude changes would do to improve results. Our data would be most improved by repeated rounds of measurements so that a better idea of the spread of our data could be qualified.

Fit	**χ^2/NDOF**
Resistance-Dependent Johnson Noise	0.1598
Frequency-Dependent Johnson Noise	11.20
Boltzmann's Constant	0.08774

TABLE III. Chi-squared values for each fit.

Component	**Uncertainty**
Octave Resistor Values	$0.3\% + 1$ LSD
BEXT, CEXT	$0.9\% + 1$ LSD
Total Bandwidth	0.02%
Preamplifier Gain (G_1)	Computed as a ratio of resistances with $0.3\% + 1$ LSD
Primary Gain (G_2)	0.01%
Squarer Output	0.02%
Fluke 179 V^2 Reading	$0.09\% + 1$ LSD

TABLE IV. Uncertainty of equipment used.

[1] J. B. Johnson, Thermal Agitation of Electricity in Conductors, Physical Review **32**, 97 (1928).
[2] TeachSpin, Inc., *Noise Fundamentals*, TeachSpin, Inc., Buffalo, NY (2010).
[3] M. Giordano, Uncertainty propagation with functionally correlated quantities, ArXiv e-prints (2016), arXiv:1610.08716 [physics.data-an].